LA-UR - 83 - 3062

LA-UR--83-3062

DE84 001729

CONF-8310143--21

TITLE: THREE-DIMENSIONAL THERMAL-HYDRAULIC CALCULATIONS USING SOLA-PTS

AUTHOR(S) Bart J Daly and Martin D. Torrey

SUBMITTED TO 11th Water Reactor Safety Research Information Meeting
National Bureau of Standards
Gaithersburg, MD
October 24-28, 1983

Los Alamos National Laboratory
Los Alamos, New Mexico 87545

FORM NO 836 R4
ST NO 2629 5/81

MASTER

THREE-DIMENSIONAL THERMAL-HYDRAULIC CALCULATIONS USING SOLA-PTS

Bart J. Daly and Martin D. Torrey
Theoretical Division, Group T-3
Los Alamos National Laboratory
Los Alamos, NM 87545

ABSTRACT

The transient, three-dimensional SOLA-PTS code has been used to study the thermal-hydraulic mixing of HPI and ambient fluids in the cold leg and downcomer with application to the pressurized thermal-shock problem. Comparisons of calculated results with 1/5th-scale experimental data are presented and shown to be in good agreement. Also shown are results obtained at full scale for a Combustion Engineering plant following an assumed main-streamline-break accident.

I. INTRODUCTION

When emergency core coolant fluid is injected into a pressurized water reactor as a consequence of a reactor accident, the reactor vessel wall may be cooled sufficiently to cause crack propagation in the metal. The likelihood of crack propagation increases with reactor age as a result of neutron flux weakening of the wall material, particularly the weldments. The analysis of crack growth, given the wall temperature and fluid pressure histories, is a fracture mechanics problem. The determination of the temperature and pressure histories requires a transient solution for the fluid-thermal mixing throughout the primary, and possibly secondary, systems using a systems code, such as TRAC[1] or RELAP5[2]. However, these systems code calculations are of necessity coarsely noded, so that they cannot compute the details of the fluid-thermal mixing in the cold legs and downcomer of the reactor. Therefore, these systems studies must be supplemented by finer-zoned, multidimensional calculations that can compute the mixing in the cold legs and downcomer and the resulting fluid temperature in the immediate vicinity of the vessel weldments.

The SOLA-PTS code[3] is a transient, three-dimensional, single-phase, incompressible numerical scheme that was designed to perform these detailed mixing calculations. The calculations, while efficient, are nevertheless lengthy, so they are only performed at isolated times during a transient when the systems code solution indicates a potential for significant cooling of the vessel wall. Then, using the systems code values of flow rates and fluid temperatures as boundary conditions at all entrances to the cold leg and downcomer, a SOLA-PTS calculation is performed. The results of

this calculation provide more realistic values of the fluid temperature at vessel weldments than can be obtained with the systems code.

Section II provides a brief description of the SOLA-PTS code. Comparisons of calculated results with experimental data from Creare R&D, Inc.[4] are presented in Sec. III. Section IV is concerned with the application of the method to a specific reactor geometry.

II. THE NUMERICAL METHOD

The SOLA-PTS code has been described previously[3] and will be documented more completely in a forthcoming paper, so only a brief general description is provided here.

The SOLA-PTS algorithm involves the solution of the continuity equation and transport equations for momentum, fluid temperature, turbulence energy k, turbulence energy decay rate ε, and the square of the fluctuating temperature field $\overline{T'^2}$. These transport equations are solved using the second-order Tensor Viscosity method[5], which is supplemented by the Filtering Remedy and Methodology (FRAM)[6] procedure for reducing dispersion errors. A preconditioned Conjugate Residual iteration scheme[7], which permits rapid convergence, is used to compute the pressure field.

A thermal diffusion equation for the metal is also included in the model, but it has not been employed in the examples presented in this paper, in which an adiabatic wall treatment has been used.

Two different turbulence models are used in SOLA-PTS to represent the diffusion of momentum and heat. In buoyant jet regions, such as the HPI inlet and the downcomer, the three equation k-ε-$\overline{T'^2}$ model of Chen and Rodi[8] is used, while in the cold leg pipe away from the HPI inlet the Launder-Spalding k-ε model[9] is used. The use of the Chen and Rodi model produces

much more mixing of warm ambient fluid with the cold HPI fluid than is obtained with the Launder-Spalding model. As will be shown in the examples presented below, this increased mixing results in excellent agreemnt between the calculated temperatures and experimental thermocouple data.

The cold leg, downcomer, lower plenum, and core are treated as a single flow region in SOLA-PTS, with the cold leg modeled as a square duct in this rectangular coordinate system. A variable computation mesh is used, with fine zoning near the HPI inlet and the junction of the cold leg and downcomer, and relatively coarser zoning elsewhere. Consistent with the variable computation mesh, all advection terms in the transport equations are differenced in nonconservative form to insure the maintenance of a higher-order accurate numerical algorithm. The accuracy of this scheme is controlled by requiring that the net flow through various planes in the computation region agree within one per cent. Computational accuracy can be improved by decreasing the pressure iteration convergence criterion.

III. EXPERIMENTAL COMPARISONS

SOLA-PTS calculations have been performed to compare with 1/5th scale experimental data obtained by Creare R&D, Inc.[4] Various Creare tests have been carried out to examine thermal-hydraulic mixing in a cold leg and downcomer for geometries that approximately model Westinghouse, Babcock and Wilcox, and Combustion Engineering designs. We present comparisons of calculated results with Creare data[4] for test 50, which used a Combustion Engineering-type design and examined the flow of HPI fluid at 64°F into stagnant ambient fluid at approximately 150°F. The HPI fluid was injected at 4.0 gal/min through a 2 inch i.d. pipe mounted at a 60° angle to a 5.625 inch i.d. cold leg pipe. Thermocouples were located along the bottom of

the cold leg, on several racks spanning the cold leg, and throughout the downcomer.

Figure 1 shows a velocity vector plot in a vertical plane through the centerline of the cold leg. The large vertical vectors in the cold leg indicate the HPI fluid entering the cold leg. This HPI fluid, which has been warmed by mixing at the injection region, flows along the bottom of the cold leg to the downcomer where it bridges the gap to impact on the core barrel wall. It then falls under gravity to the bottom of the downcomer, and flows through the lower plenum to the core. The volume of fluid exiting from the top of the core exactly matches that entering at the HPI inlet. Return warm water flows from the downcomer along the top of the cold leg to mix with the HPI fluid at the injection region.

Each velocity vector in Fig. 1 corresponds to a SOLA-PTS computation cell. Thus, this figure gives an indication of the mesh resolution in the calculation, which is finest at the cold leg-downcomer junction and at the HPI inlet, and coarsest at the end of the cold leg and in the core. Notice the expansion of the downcomer gap below the cold leg junction.

A velocity vector plot in a horizontal plane through the bottom of the cold leg is shown in Fig. 2. Notice the impaction point below the HPI injection port and the spreading of the flow upstream and downstream from this point. When the fluid reaches the downcomer, it spreads asymmetrically with the greatest flow away from the hot leg obstruction, which occupies the region without vectors on the right side of the downcomer. A corresponding velocity vector plot in a horizontal plane through the top of the cold leg would show that the warm water return flow into the cold leg enters from the hot leg side. These flow patterns are controlled by the flow

circulations that develop in the downcomer as a consequence of buoyancy and convective forces.

Figures 3-12 show comparisons of calculated and experimental temperature measurements during the first 200 sec of the test. The schematic inset in each figure shows the location of the thermocouple. Figure 3 shows the temperature of fluid that has splashed upstream from the HPI inlet along the bottom of the cold leg. The calculated results are in excellent agreement with the data throughout the transient. Notice that the fluid temperature in the calculation is 150°F initially; this value was used throughout the fluid. However, the initial temperature in the experiment varied from 148°F to 152°F, so there will be some discrepancies between calculation and experiment in the starting values.

The most rapid temperature drop occurs directly below the HPI injection port as shown in Fig. 4. The experimental data are highly oscillatory because of the turbulent nature of the flow in this region and the unstable temperature field below the inlet. Of course, the turbulent oscillations cannot be reproduced in the calculation, which resolves the turbulence only in an average sense. Again, the calculation and the experiment are in excellent agreement, although the calculation shows a slightly cooler temperature at late times. This good agreement persists in the cold leg, as shown in Fig. 5 for a point approximately midway between the HPI inlet and the downcomer.

Figures 6-10 show comparisons of the calculated and experimental results at uniform intervals across the cold leg at a point near the downcomer junction. For thermocouple locations such as these that are not located on the cold leg wall, an adjustment must be made to account for the

square cross section of the cold leg in the calculation. We do this by interpolating the temperature to a height that is proportional to the center of area of the measurement in the experiment.

The calculated and experimental plots in Figs. 6-10 show a strong temperature gradient across the cold leg. The results are in good agreement, except in Fig. 8 where the thermocouple is located in the middle of the cold leg. The calculated value is in the cold fluid region while the experimental measurement is in the upper hotter fluid. It is clear from the large oscillations in the experimental data that this thermocouple is located very close to the thermal interface. However, it also appears that the cold fluid layer is thicker in the calculations than in the experiments. This is consistent with the slightly greater travel time of the cold layer in the calculations as shown by the later arrival time in Fig. 6.

Figures 11 and 12 show the fluid temperatures in the downcomer just below the junction with the cold leg on the vessel and core barrel walls, respectively. In both figures, the calculation and experiment are in good agreement, although the experimental data exhibit large turbulent fluctuations that are averaged out by the turbulence model in the calculation. A comparison of the two figures shows a qualitative difference in the temperature history at the two locations. On the core barrel wall there is a large initial temperature drop followed by a steady decline, which is interrupted by some short-lived temperature fluctuations after 140 sec in the experimental plot. On the vessel side, Fig. 11, there is an initial temperature drop, but then a temperature recovery before the gradual thermal decline. This indicates a relatively greater buoyant mixing on the vessel

side due to the smaller inertial forces and lower pressure there. This asymmetrical cooling gradually decreases with depth in the downcomer. Near the bottom of the downcomer the temperature transients are similar in appearance; they both exhibit an initial temperature drop, followed by a recovery, and then a gradual thermal decline.

IV. PLANT SPECIFIC APPLICATION

We have applied the SOLA-PTS code to the analysis of fluid-thermal mixing for the Calvert Cliffs 1 plant, using data obtained in a TRAC calculation[10] for the specification of boundary conditions. Calvert Cliffs 1 is a Combustion Engineering plant of a design that is similar to the 1/5th scale Creare experiment for which comparisons have been presented above. The TRAC study examined the transient consequences of a postulated main streamline break from hot zero power. The results of the TRAC calculation showed that there was no loop flow into the intact cold legs after about 300 sec following the streamline break. Since there is significant HPI and charging flow into the cold legs during the time period 150-800 sec, the potential for significant cooling of the vessel wall does exist for this assumed scenario. However, this cooling tendency may be offset by the fact that a small, but not insignificant, flow is maintained on the broken loop side. Indeed, the TRAC calculation[10] shows that, because of this broken loop flow, the downcomer temperature does not drop below 250°F, except for a brief oscillation.

As a first step in a detailed analysis of these flow conditions, we have used the SOLA-PTS code[3] to examine three-dimensional interactions at 385 sec into the transient for a 90° section of the downcomer on the intact loop side. At this time, the TRAC calculation showed that HPI fluid was flowing into the cold leg at a rate of 13.03 kg/s and at a temperature of

285.9K (55°F), the charging flow was 4.15 kg/s at a temperature of 302.6K (85°F), and the average temperature in the downcomer and cold leg was approximately 443.7K (339°F). These conditions were used to set the boundary conditions for the SOLA-PTS calculation. We plan to perform additional calculations in which the inlet flow rates and temperatures are varied in accordance with the TRAC calculations for 90° and 180° segments of the downcomer to examine transient and azimuthal mixing effects. However, this first calculation with steady boundary conditions corresponds more directly with the Creare experimental conditions, so we can examine the consistency of the calculated results with those obtained for the 1/5th scale comparisons.

Figures 13-15 show the temperatures measured at vessel weld locations below the centerline of the cold leg and at locations displaced 13 cm azimuthally on each side of the centerline. These locations correspond approximately to that of thermocouple 7 of the 1/5th scale study shown in Fig. 11. As in that figure, the temperatures in Figs. 13-15 show an initial drop when the cool water from the cold leg reaches that location, then a temperature recovery followed by a gradual thermal decline. These figures indicate that the cold water flow is not symmetric about the cold leg centerline, and this trend is also apparent in the 1/5th scale data and calculations. Thus, these full scale calculations are consistent with the small scale results. The thermal decay rate following the temperature recovery in Figs. 13-15 is approximately 0.4°F/sec. However, it must be emphasized that these results were obtained in a calculation that neglected transient and azimuthal mixing effects, and therefore are probably conservative. In addition, this postulated accident scenario neglects operator intervention.

Figure 16 shows a velocity vector plot at an early time in a transient calculation for a 180° downcomer segment. We will examine the detailed mixing of HPI and charging flows with the ambient fluid in the intact cold leg, but will assume thorough mixing in the broken loop cold leg. This assumption is justified by the fact that the broken loop flow rate is approximately an order of magnitude greater than that of the combined HPI and charging flows. Also, since the fluid temperature in the cold leg on the broken loop side is greater than the downcomer temperature, we assume that there is no countercurrent flow in that cold leg and inject the thoroughly mixed cold leg flow directly into the downcomer. This appears as the high velocity flow at the left of the figure. Calculations for this 180° downcomer segment are in progress at the present time.

REFERENCES

1. "TRAC-PF1/MOD1, An Advanced Best Estimate Computer Program for Pressurized Water Reactor Analysis," Los Alamos National Laboratory report (to be published).

2. V. H. Ransom et al., "RELAP5/MOD1 Code Manual," Vols. 1&2, NUREG/CR-1826, EGG-2070, March 1982.

3. B. J. Daly, B. A. Kashiwa, and M. D. Torrey, "Calculations of Pressurized Thermal Shock Problems with the SOLA-PTS Method," Proc. of the Tenth Water Reactor Safety Research Information Meeting, October 12-15, 1982, p. 113.

4. P. H. Rothe and M. F. Ackerson, "Fluid and Thermal Mixing in a Model Cold Leg and Downcomer with Loop Flow," EPRI report NP-2312, April 1982.

5. J. K. Dukowicz and J. D. Ramshaw, "Tensor Viscosity Method for Convection in Numerical Fluid Dynamics," J. Comput. Phys. 32, 71, July 1979.

6. M. Chapman, "FRAM: Nonlinear Damping Algorithms for the Continuity Equation," J. Comput. Phys. 44, 84, 1981.

7. R. Chandra, "Conjugate Gradient Methods for Partial Differential Equations," Ph.D. Thesis, Yale University, 1978.

8. C. J. Chen and W. Rodi, "A Mathematical Model for Stratified Turbulent Flow and its Application to Buoyant Jets," 16th IAHR Congress, Section C.a, San Paulo, Brazil, 1975.

9. B. E. Launder and D. B. Spalding, "The Numerical Computation of Turbulent Flows," Comput. Meth. in Appl. Mech. and Eng. 3, 269, 1974.

10. J. Koenig, "PTS Accident Analysis for a CE Plant Using TRAC PF1," Proc. of the 11th Water Reactor Safety Research Information Meeting.

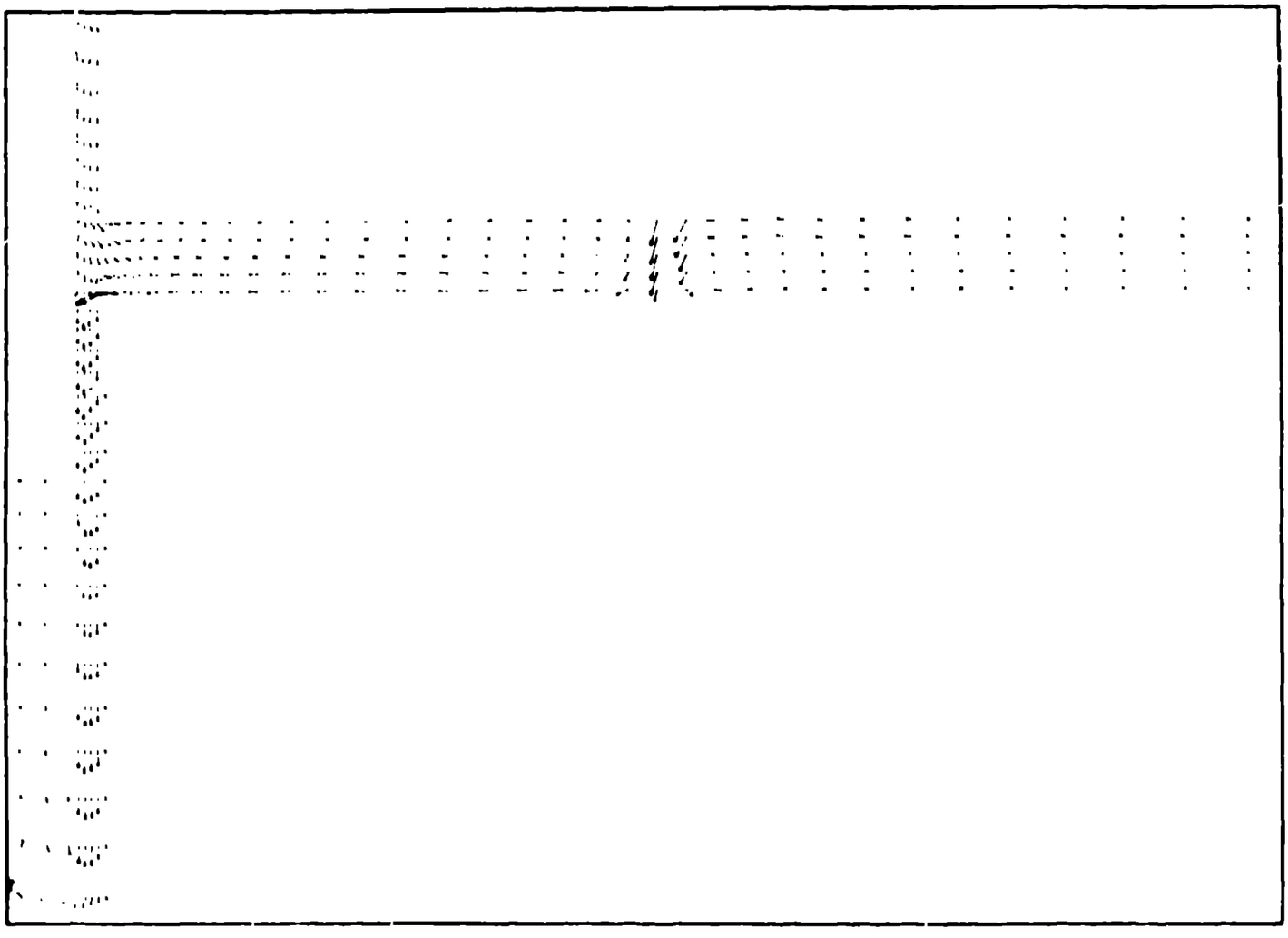

Fig. 1. A velocity vector plot in a vertical plane through the centerline of the cold leg. From left to right the flow regions are the core, the downcomer and lower plenum, and the cold leg. The large vertical vectors in the cold leg show the HPI fluid entering the cold leg. In this zero loop flow problem the HPI flow separates when it impacts on the bottom of the cold leg; part flows upstream in a circulating flow and part flows downstream toward the downcomer. The flow from the cold leg jumps the downcomer gap to impact on the core barrel wall.

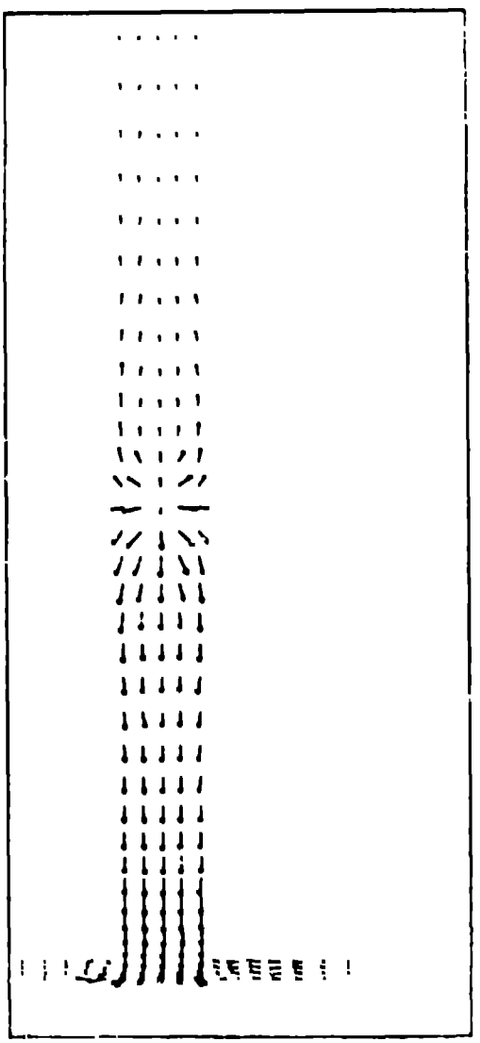

Fig. 2. A velocity vector plot in a horizontal plane through the bottom of the cold leg. Note the impact region of the HPI flow. The fluid flows into the downcomer in an asymmetric fashion with the principal flow in this plane being in a direction away from the hot leg obstacle, which occupies the region without vectors at the right side of the figure.

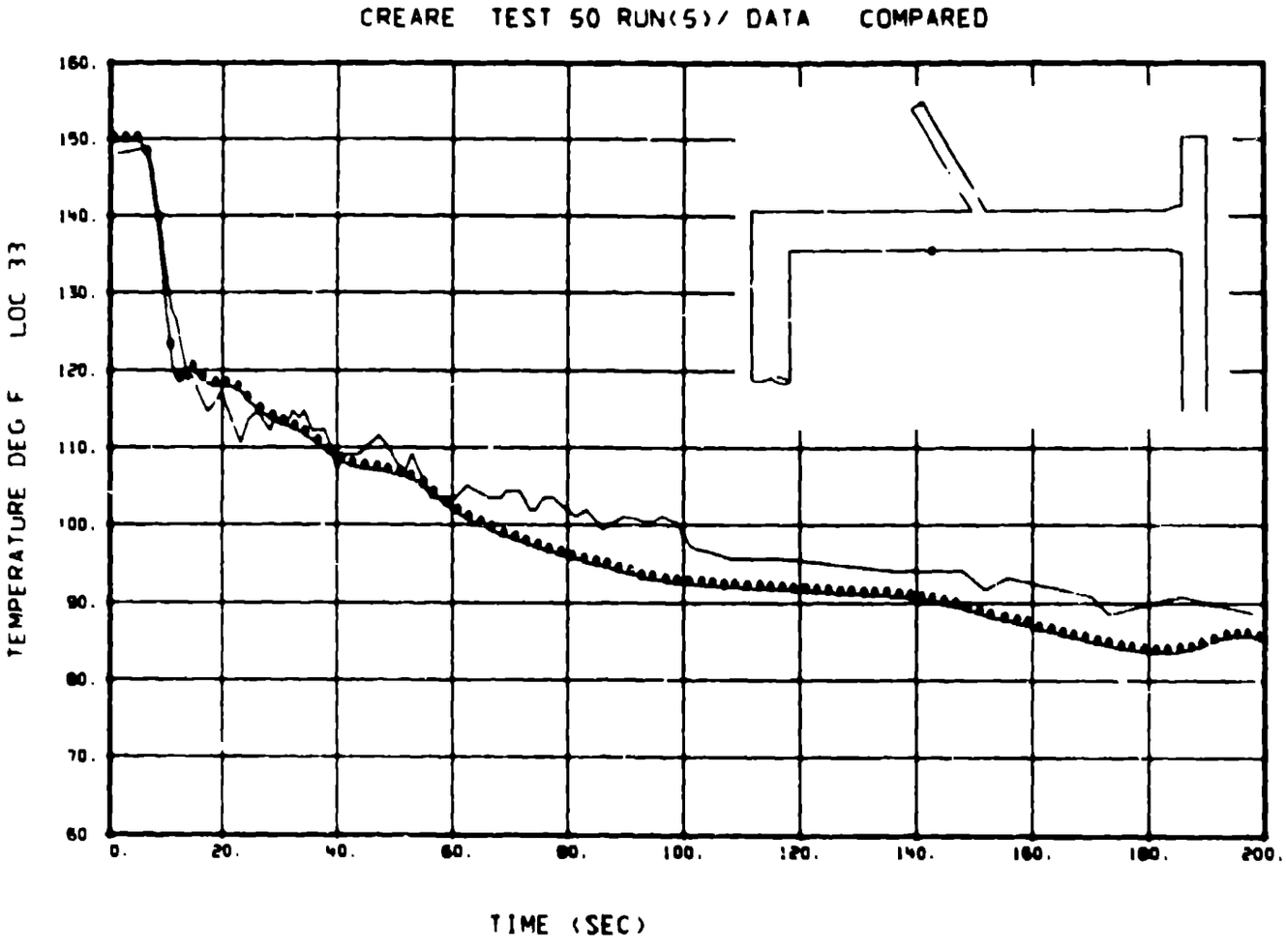

Fig. 3. A comparison of calculated (the line with the datum points) and experimental temperature measurements for Creare test 50 at thermocouple 33, which is located at the bottom of the cold leg, on the centerline, upstream from the HPI injection pipe.

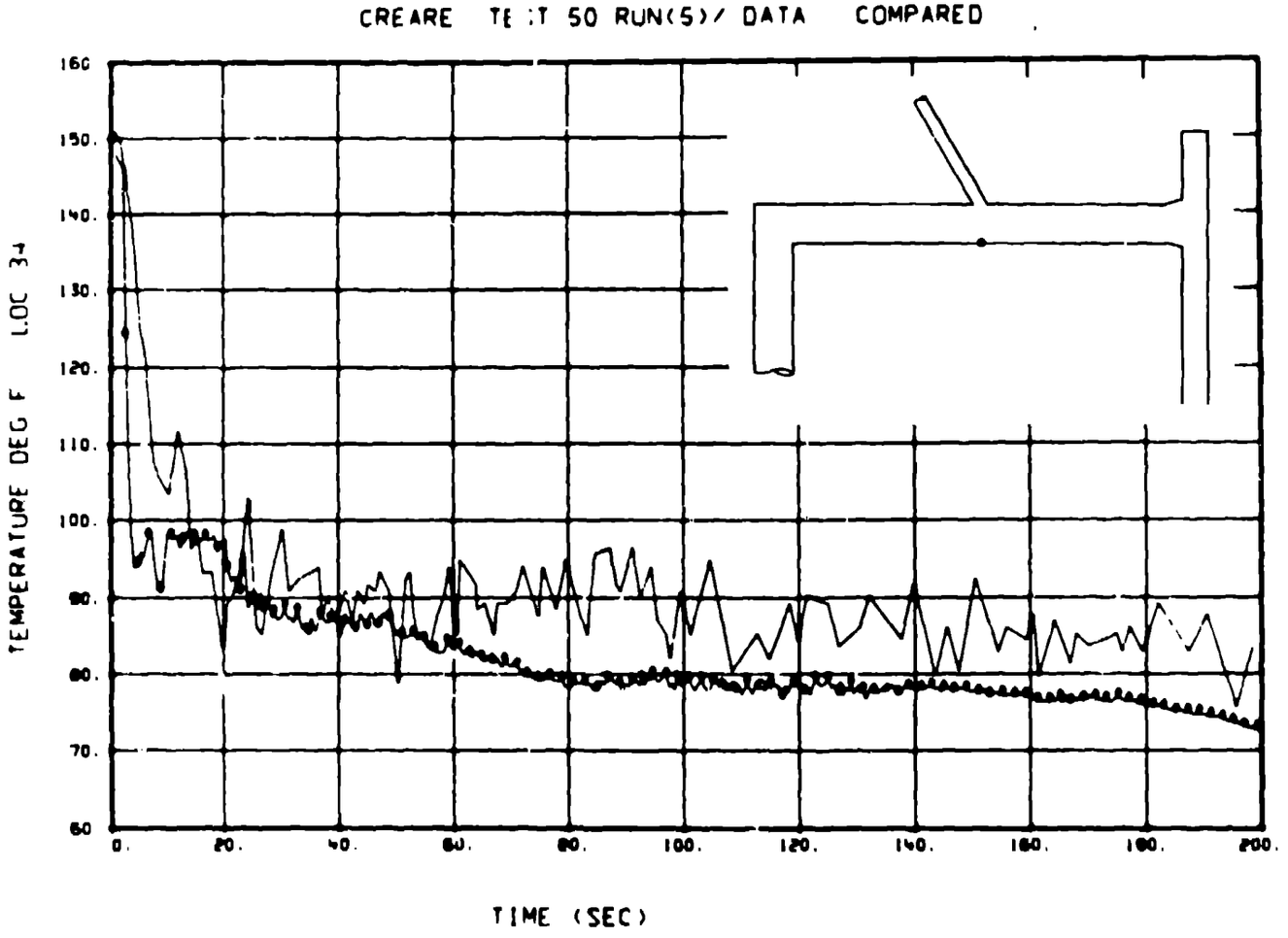

Fig. 4. A comparison of calculated (the line with the datum points) and experimental temperature measurements for Creare test 50 at thermocouple 34, which is located at the bottom of the cold leg, on the centerline, directly under the HPI injection pipe. The experimental data is highly oscillatory because of the turbulent nature of the flow in this region and the unstable temperature field below the inlet.

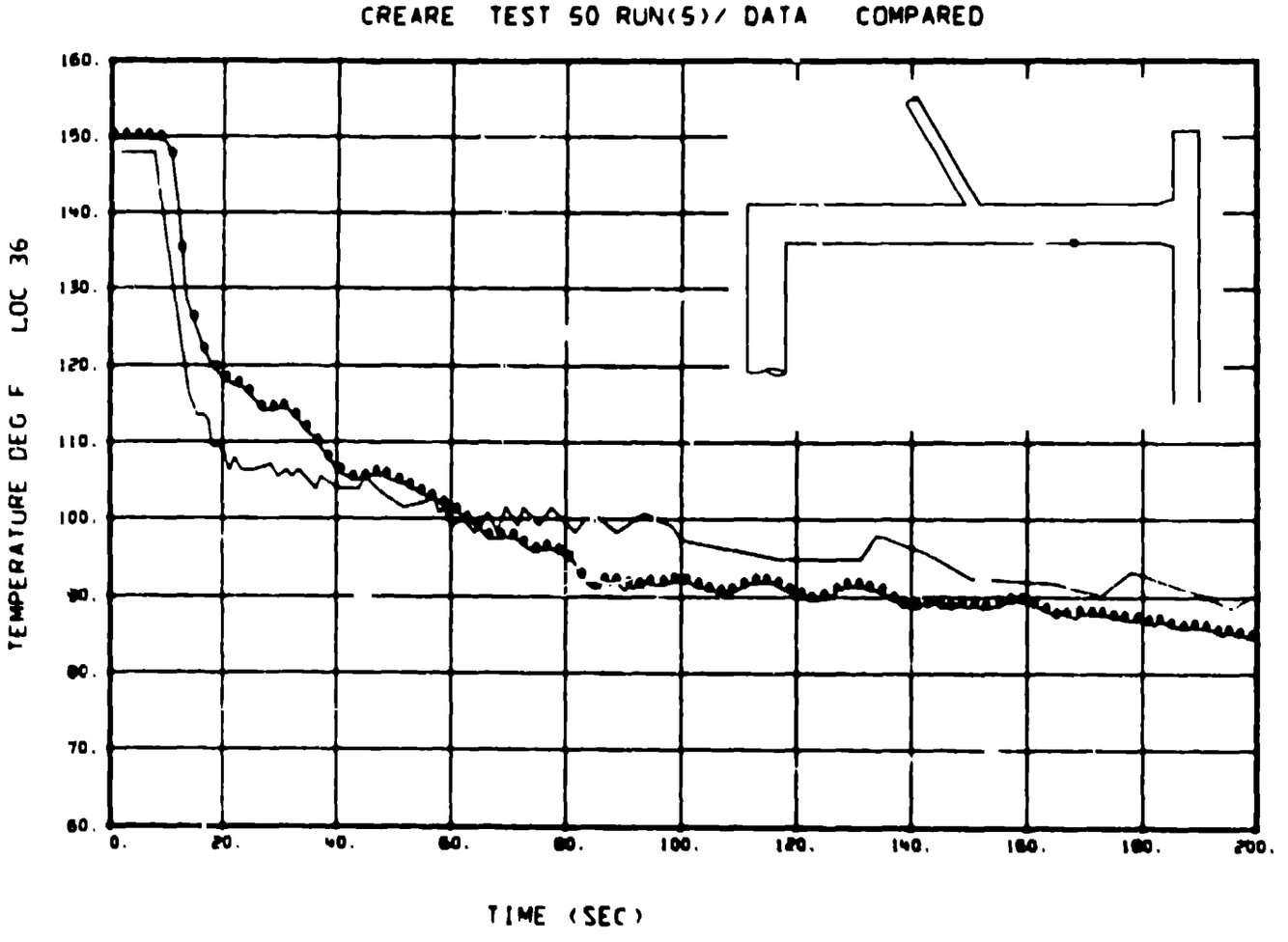

Fig. 5. A comparison of calculated (the line with the datum points) and experimental temperature measurements for Creare test 50 at thermocouple 36, which is located at the bottom of the cold leg, on the centerline, downstream from the HPI injection pipe.

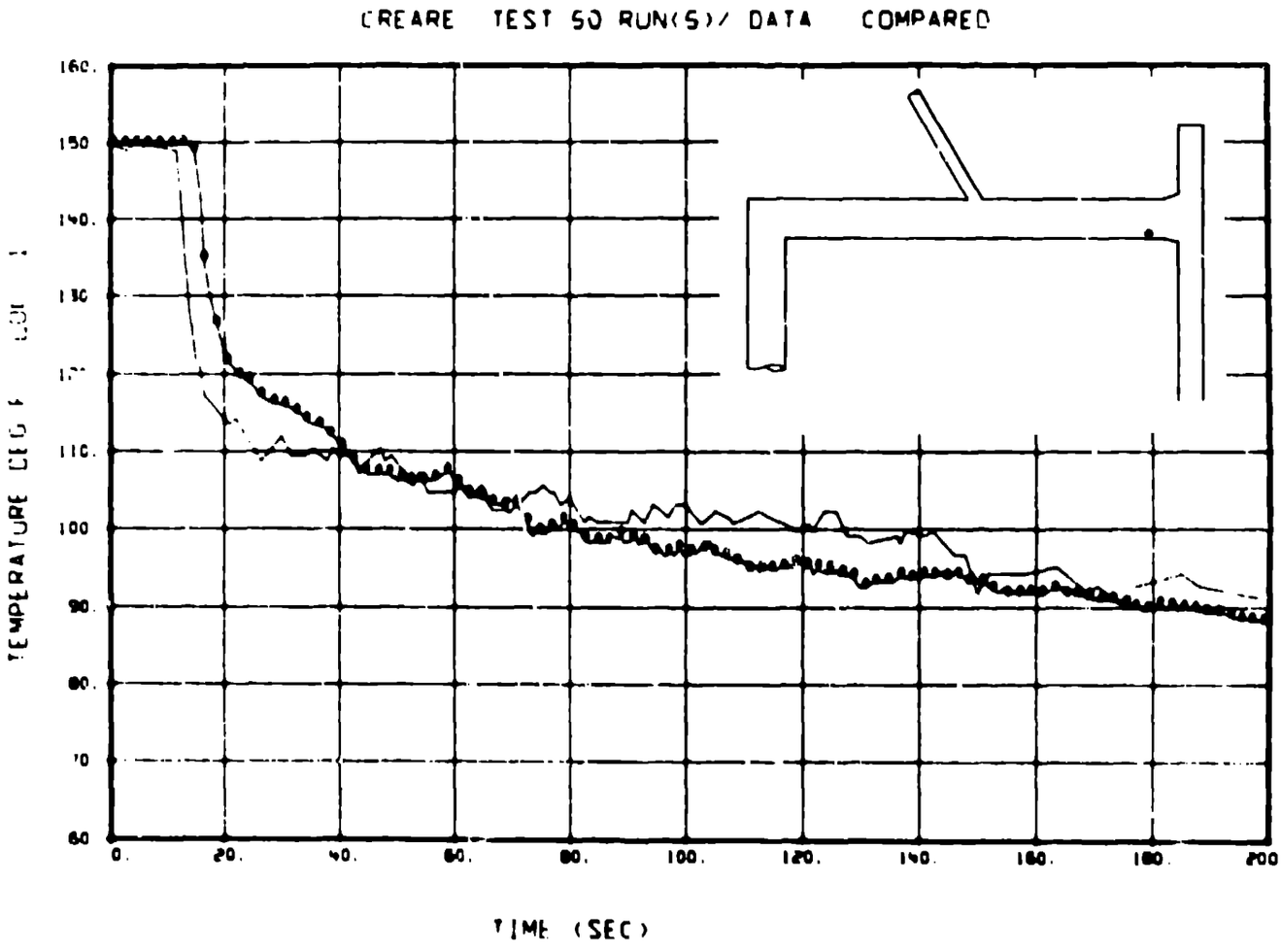

Fig. 6. A comparison of calculated (the line with the datum points) and experimental temperature measurements for Creare test 50 at thermocouple 1, which is located 1.0 cm above the bottom of the cold leg, on the centerline, and 12.0 cm from the juncture with the downcomer.

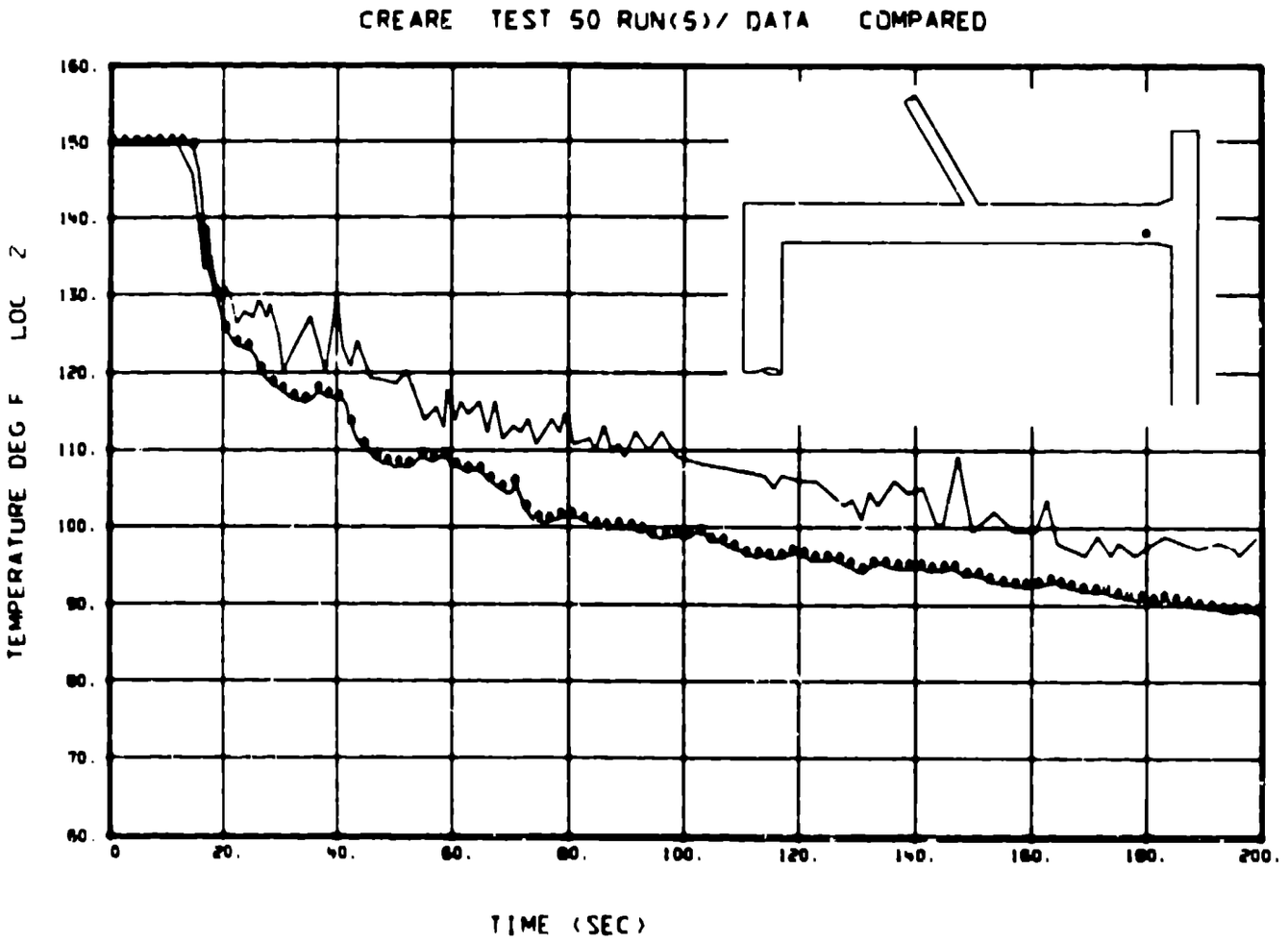

Fig. 7. A comparison of calculated (the line with the datum points) and experimental temperature measurements for Creare test 50 at thermocouple 2, which is located 4.0 cm above the bottom of the cold leg, on the centerline, and 12.0 cm from the juncture with the downcomer.

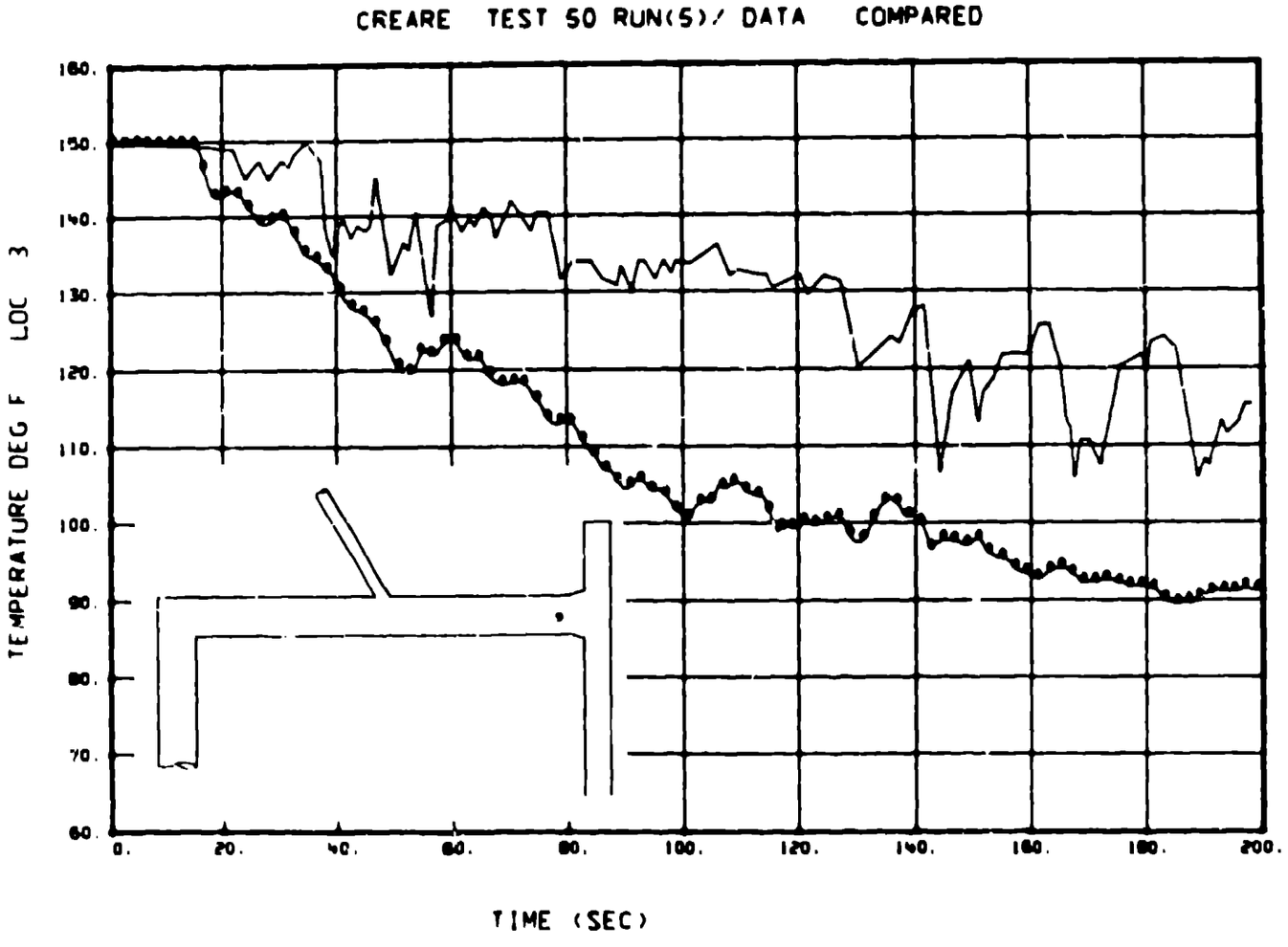

Fig. 8. A comparison of calculated (the line with the datum points) and experimental temperature measurements for Creare test 50 at thermocouple 3, which is located 4.0 cm above the bottom of the cold leg, on the centerline, and 12.0 cm from the juncture with the downcomer. This thermocouple is at the middle of the cold leg pipe. The calculated measurement is in the cold fluid region, while the experimental measurement is in the upper hotter fluid.

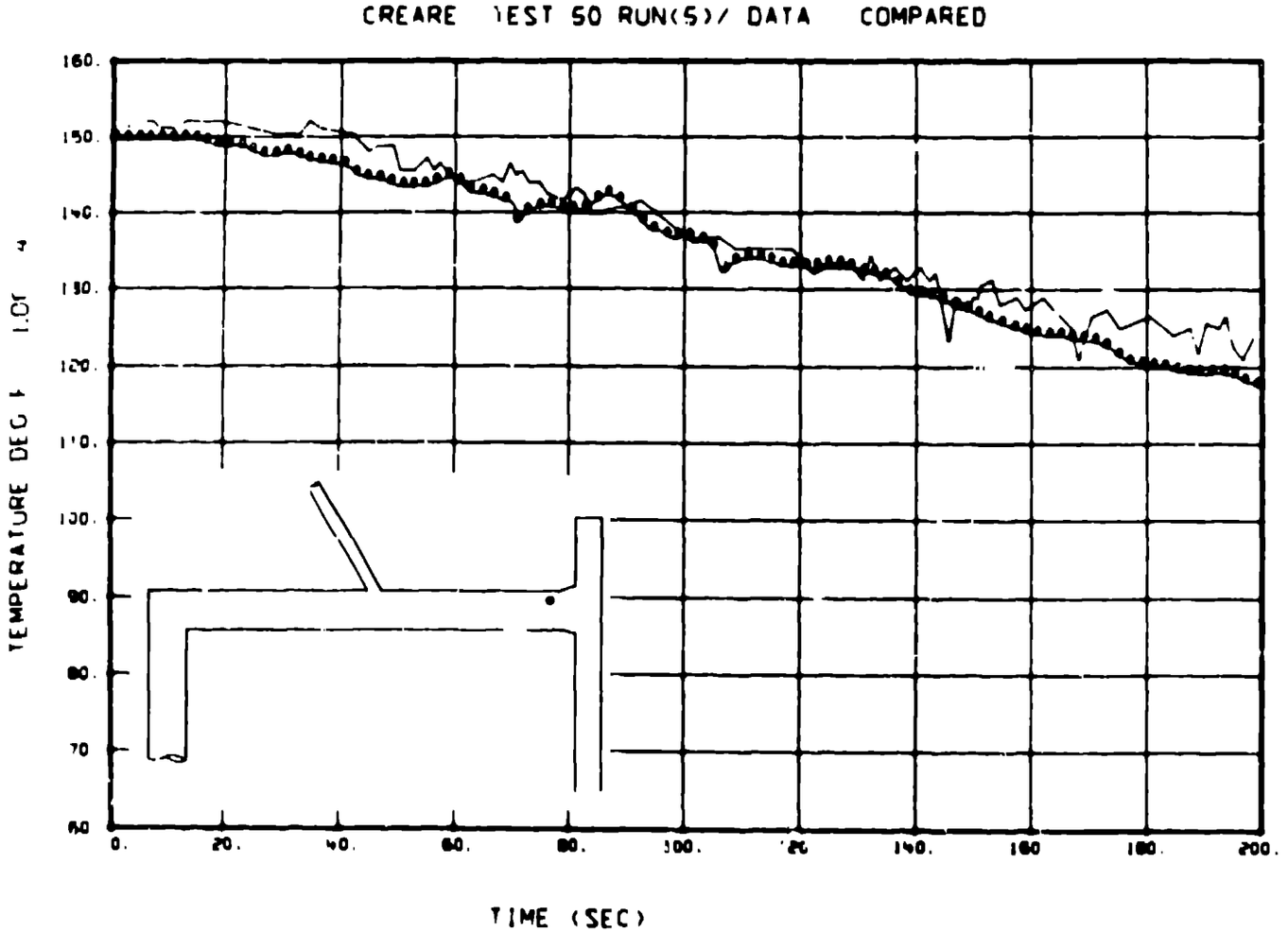

Fig. 9. A comparison of calculated (the line with the datum points) and experimental temperature measurements for Creare test 50 at thermocouple 4, which is located 10.2 cm above the bottom of the cold leg, on the centerline, and 12.0 cm from the juncture with the downcomer.

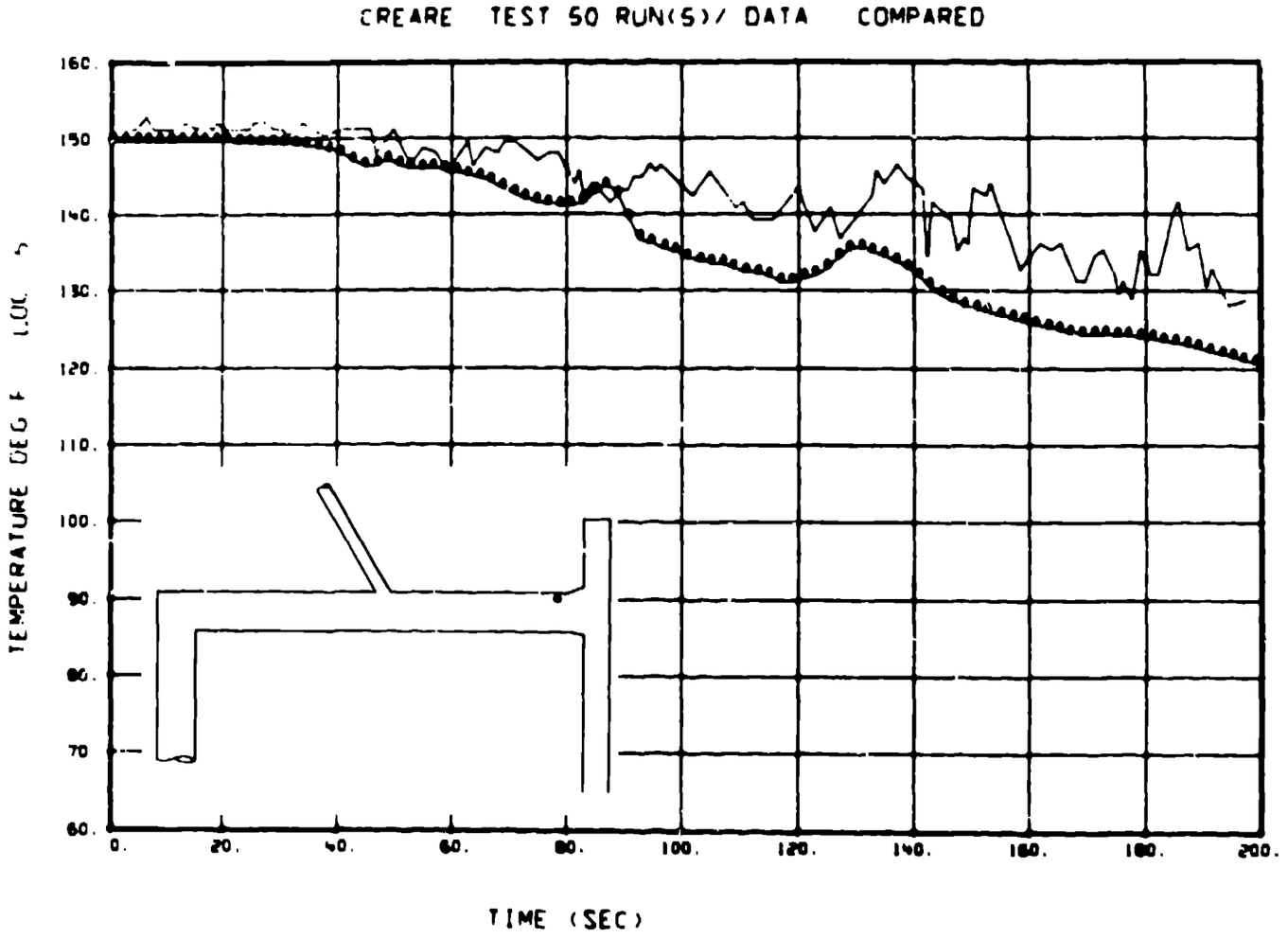

Fig. 10. A comparison of calculated (the line with the datum points) and experimental temperature measurements for Creare test 50 at thermocouple 5, which is located 13.2 cm above the bottom of the cold leg, on the centerline, and 12.0 cm from the juncture with the downcomer.

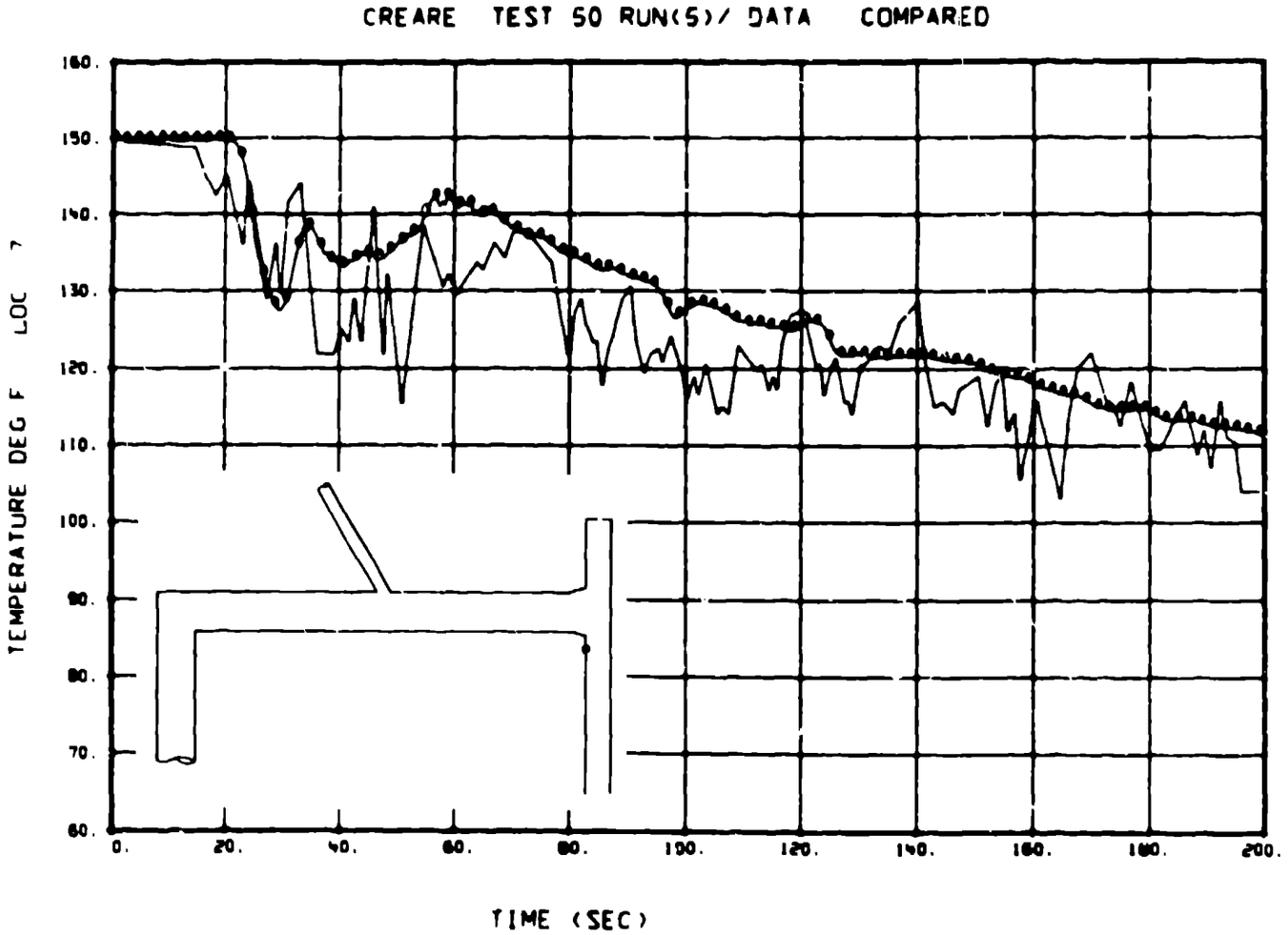

Fig. 11. A comparison of calculated (the line with the datum points) and experimental temperature measurements for Creare test 50 at thermocouple 7, which is located on the vessel wall, 10.1 cm below the bottom of the cold leg, on the cold leg centerline. Note that both the calculation and the experiment show an initial temperature drop, followed by a temperature increase, and then a gradual thermal decline.

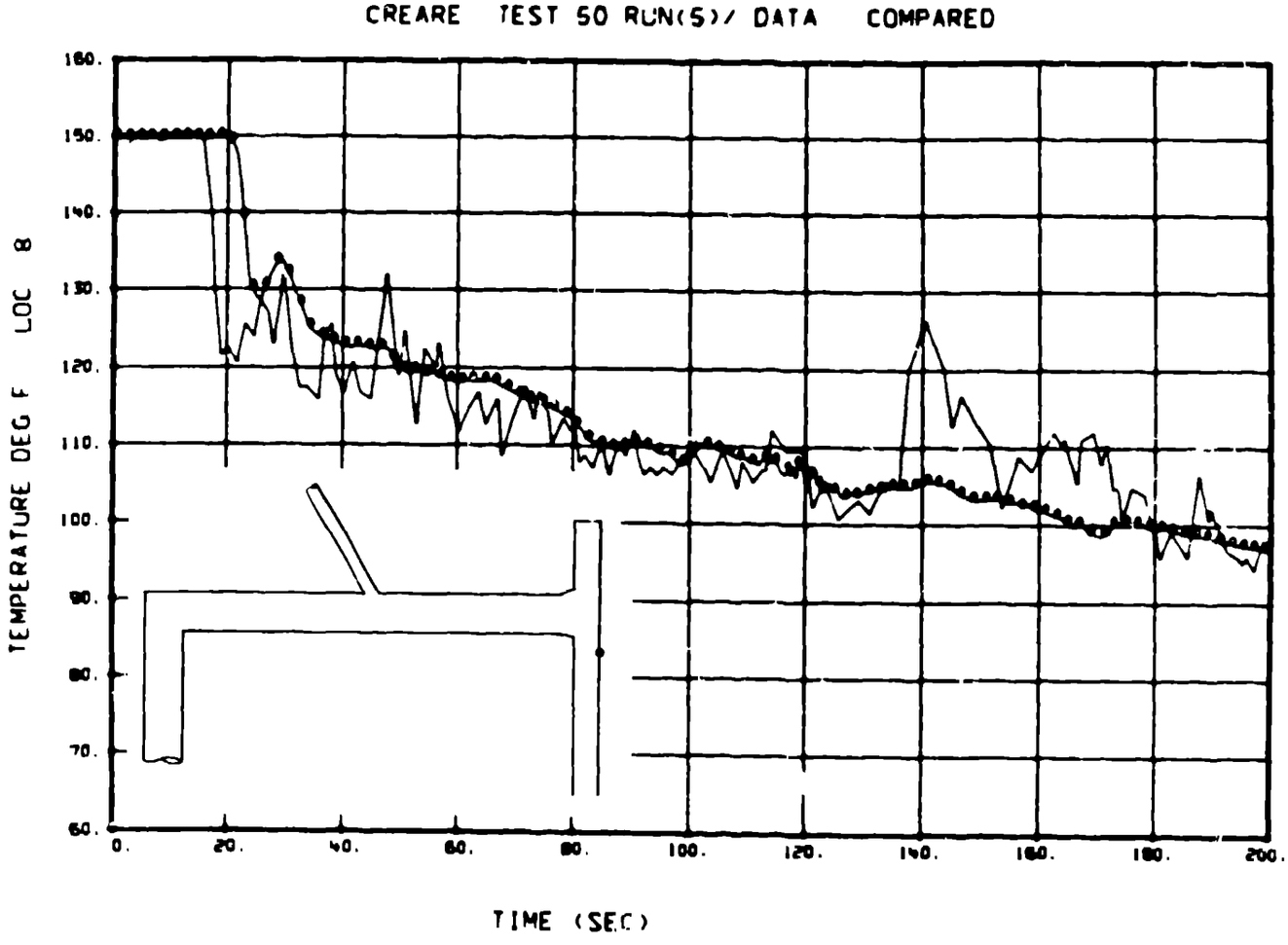

Fig. 12. A comparison of calculated (the line with the datum points) and experimental temperature measurements for Creare test 50 at thermocouple 8, which is located on the core barrel wall 12.7 cm below the bottom of the cold leg, on the cold leg centerline. Unlike thermocouple 7, there is no temperature increase following the initial temperature drop.

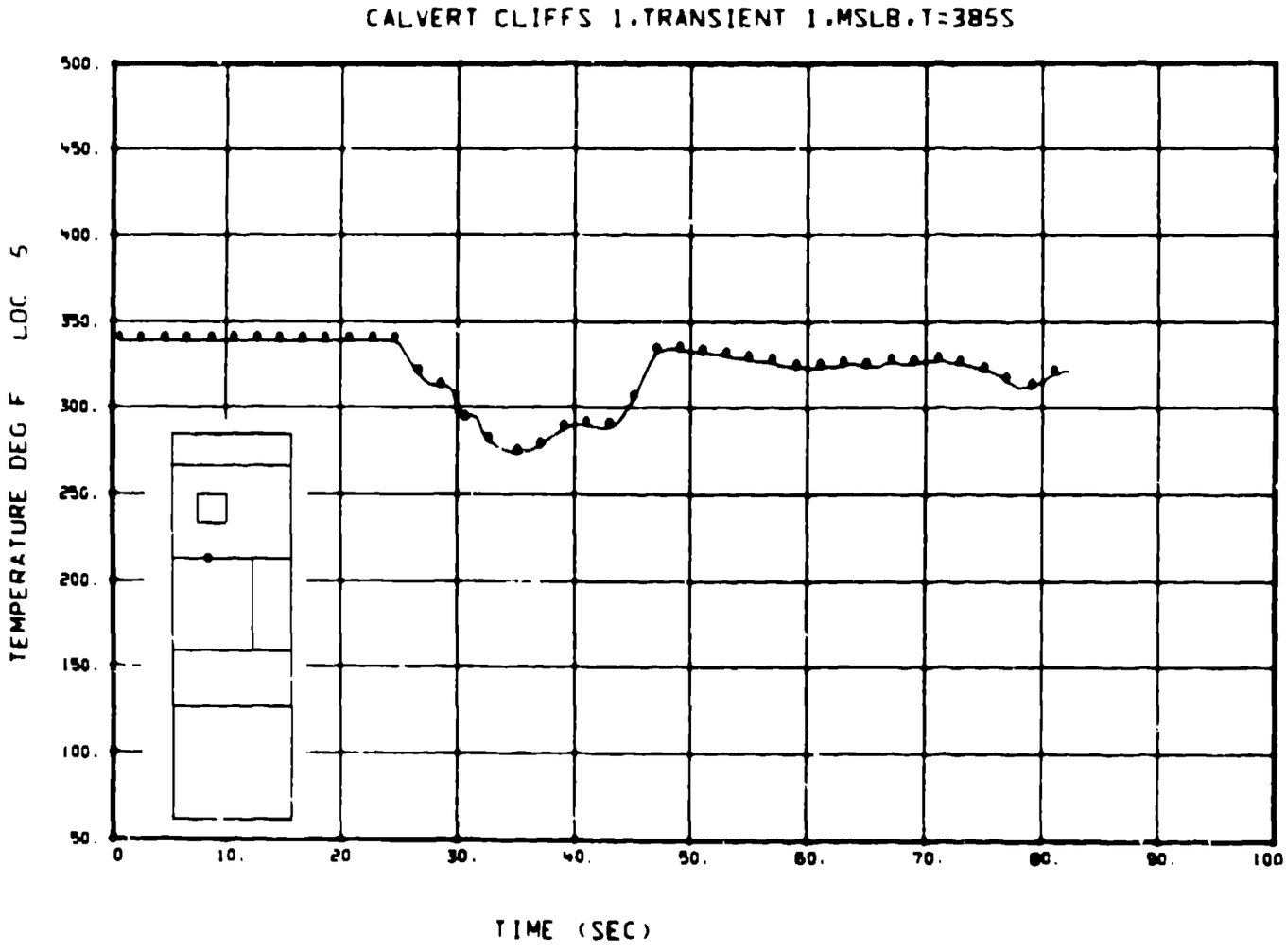

Fig. 13. The calculated temperature in a fluid cell adjacent to a vessel weld 98.3 cm below the bottom of an intact cold leg and offset 13.5 cm from the cold leg centerline as shown in the inset. This calculation used flow rates and fluid temperatures provided by a TRAC calculation of a postulated main steamline break accident in the Calvert Cliffs 1 plant.

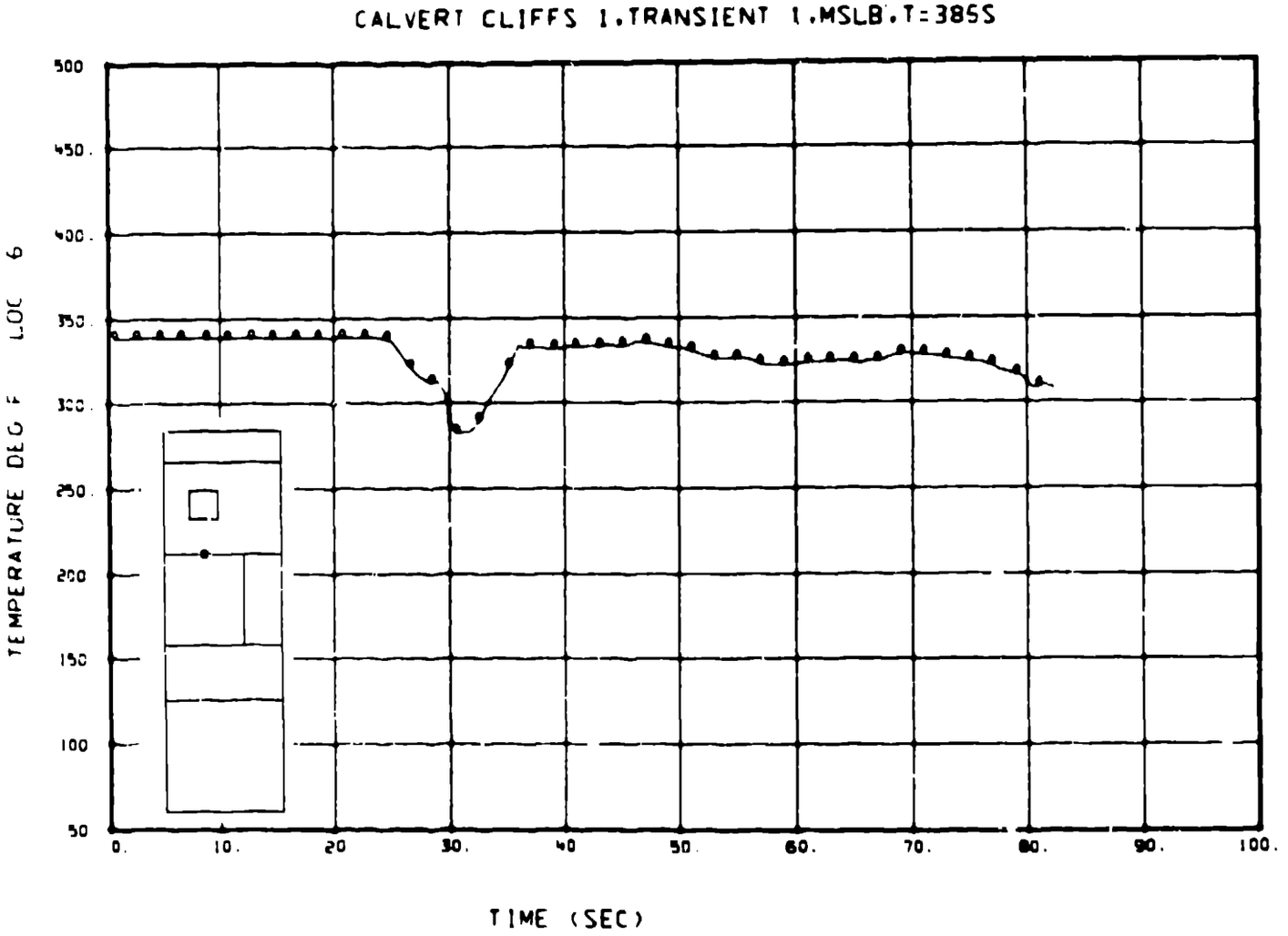

Fig. 14. The calculated temperature in a fluid cell adjacent to a vessel weld 98.3 cm below the bottom of an intact cold leg and on the cold leg centerline as shown in the inset. This calculation used flow rates and fluid temperatures provided by a TRAC calculation of a postulated main steamline break accident in the Calvert Cliffs 1 plant.

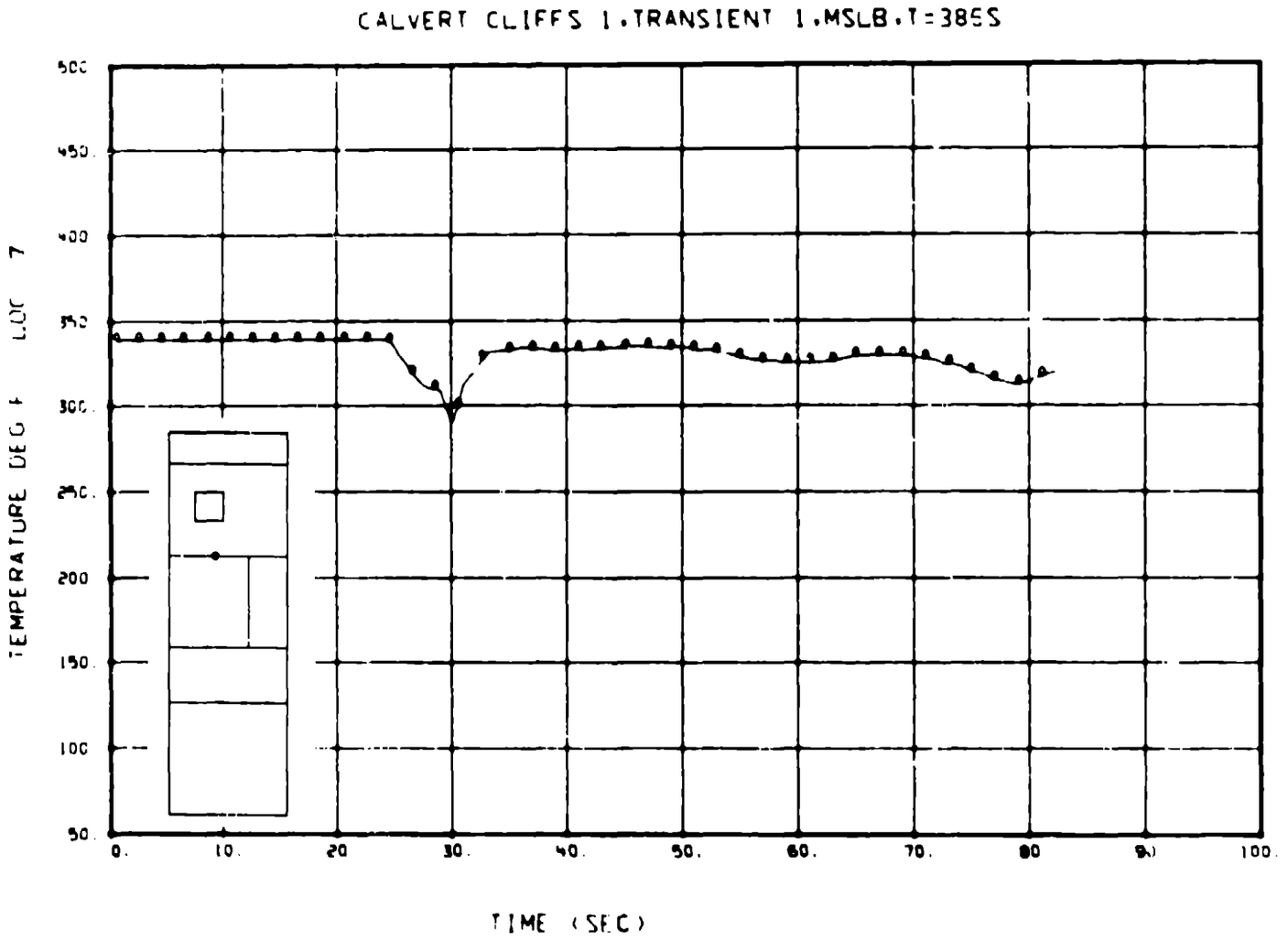

Fig. 15. The calculated temperature in a fluid cell adjacent to a vessel weld 98.3 cm below the bottom of an intact cold leg and offset 13.5 cm from the cold leg centerline as shown in the inset. This calculation used flow rates and fluid temperatures provided by a TRAC calculation of a postulated main steamline break accident in the Calvert Cliffs 1 plant.

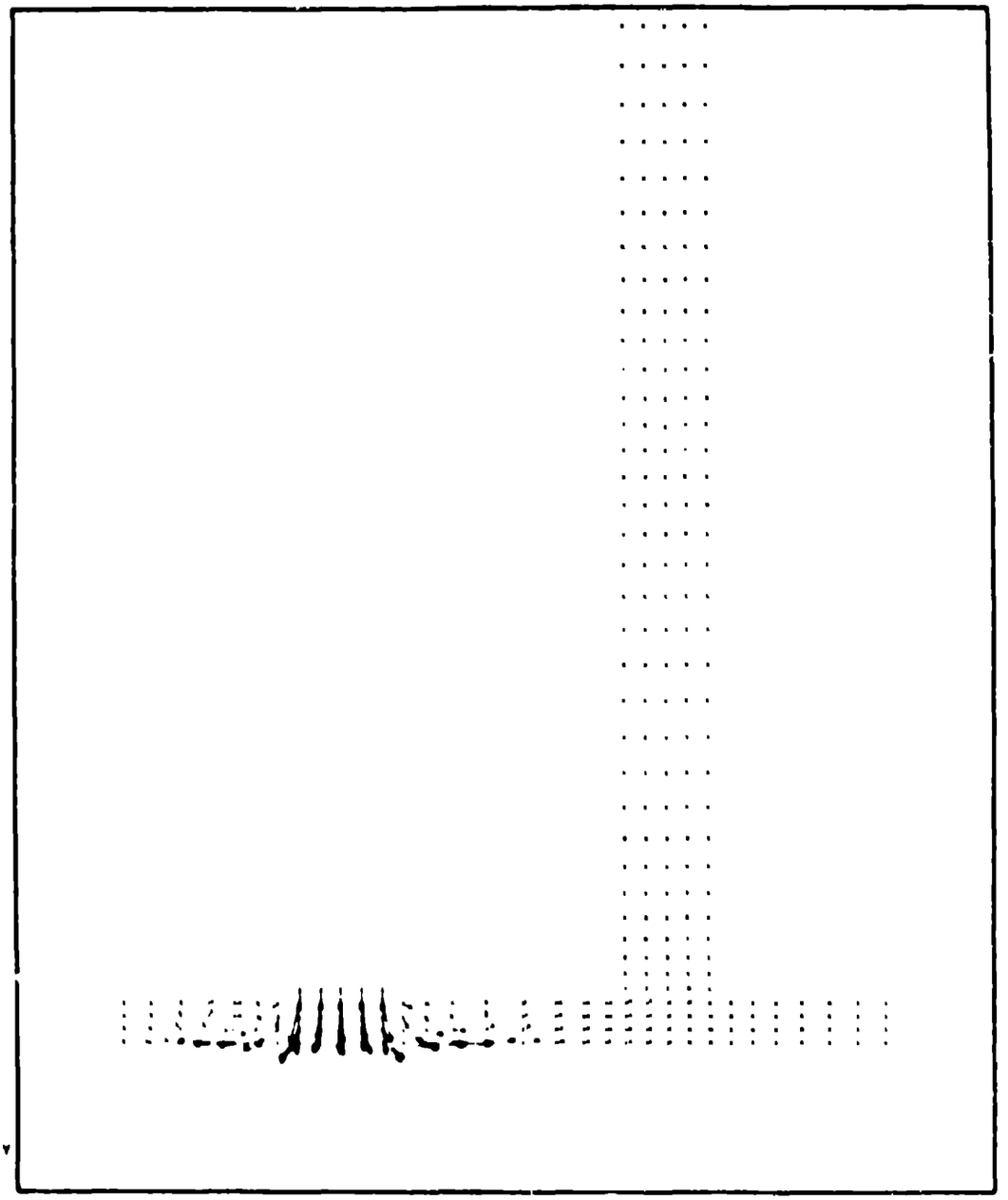

Fig. 16. A velocity vector plot in a horizontal plane through the top of the cold leg at an early time in a calculation that included a 180° downcomer segment of the Calvert Cliffs 1 plant. Only the intact loop cold leg flow is resolved in this calculation. The fluid in the broken loop cold leg is assumed to be thoroughly mixed and is injected directly into the downcomer as shown in the lower left of the figure.